

Original Article

microRNA-454 shows anti-angiogenic and anti-metastatic activity in pancreatic ductal adenocarcinoma by targeting LRP6

Yue Fan¹, Chenye Shi², Tianyu Li¹, Tiantao Kuang²

Departments of ¹Integrated TCM & Western Medicine, ²General Surgery, Zhongshan Hospital, Fudan University, Shanghai 200032, China

Received November 14, 2016; Accepted December 5, 2016; Epub January 1, 2017; Published January 15, 2017

Abstract: Our previous work has shown that microRNA-454 (miR-454) can inhibit the growth of pancreatic ductal adenocarcinoma (PDAC) by blocking the recruitment of bone marrow-derived macrophages. In the present study, we aimed to explore its role in the proliferation, invasion, and pro-angiogenic activity of PDAC cells in vitro and lung metastasis in vivo. PANC-1 and MiaPaCa-2 cells were transfected with a miR-454-expressing plasmid and tested for cell proliferation, colony formation, cell cycle distribution, invasion, and pro-angiogenic activity. The target gene(s) that mediated the action of miR-454 was identified. The effect of miR-454 overexpression on lung metastasis of PDAC was evaluated in nude mice. Of note, overexpression of miR-454 significantly inhibited PDAC cell proliferation and colony formation and arrests PDAC cells at the G2/M phase. Decreased invasiveness was observed in miR-454-overexpressing PDAC cells. Conditioned media from miR-454-overexpressing PANC-1 cells contained lower levels of vascular endothelial growth factor and had reduced capacity to induce endothelial cell tube-like structure formation. Mechanistically, miR-454 was found to target the mRNA of *LRP6* and inhibit the activation of Wnt/ β -catenin signaling in PDAC cells. Ectopic expression of *LRP6* significantly reversed the suppressive effects of miR-454 on PDAC cells. In vivo studies confirmed that miR-454-overexpressing PANC-1 cells formed significantly less lung metastases than control cells. Altogether, miR-454 functions as a suppressor in tumor growth, angiogenesis, and metastasis in PDAC, likely through downregulation of *LRP6*.

Keywords: Angiogenesis, growth, *LRP6*, metastasis, microRNA-454, pancreatic cancer

Introduction

Pancreatic ductal adenocarcinoma (PDAC) is one of the most aggressive and lethal malignancies, with an overall 5-year survival rate of less than 5% [1]. Angiogenesis plays a critical role in tumor growth and metastasis, which is responsible for supplying nutrients and oxygen [2]. Vascular endothelial growth factor (VEGF), a well-defined inducer of angiogenesis, has been reported to be abundantly expressed in PDAC specimens [3]. Preclinical studies demonstrated that targeting VEGF signaling leads to reduced tumor growth and angiogenesis in subcutaneous tumor xenografts of human PDAC [4, 5]. Better understanding the mechanisms that govern tumor angiogenesis and metastasis is of importance to develop effective therapies for PDAC.

microRNAs (miRNAs) are a family of small non-coding RNAs that can negatively regulate a large number of genes by binding to the 3'-untranslated region (UTR) of target mRNAs [6]. Dysregulation of miRNAs commonly occurs in PDAC and has been linked to tumor progression [7, 8]. For example, it was reported that miR-323-3p is underexpressed in PDAC tissues and cell lines and inhibits invasion and metastasis of PDAC cells [7]. miR-454 acts as an oncogene in several human cancers such as uveal melanoma [9] and non-small cell lung cancer [10]. Our previous work provides evidence that miR-454 is downregulated in PDAC and shows inhibitory effects on the growth of PDAC by targeting stromal cell derived factor-1 (SDF-1) [11]. Furthermore, we showed that miR-454 overexpression impairs the ability of PDACs to recruit bone marrow-derived macrophages in

transwell migration assays. However, the role of miR-454 in tumor angiogenesis and metastasis in PDAC is still unclear.

In the present study, we determined the effects of overexpression of miR-454 on the growth, cell cycle distribution, invasion, and pro-angiogenic activity of PDAC cells in vitro and lung metastasis in vivo. The target gene(s) that mediates the action of miR-454 in PDAC were also investigated.

Materials and methods

Cell lines

Human PDAC cell lines PANC-1 and MiaPaCa-2 were obtained from the American Type Culture Collection (ATCC, Rockville, MD, USA). Cells were maintained in Dulbecco's modified Eagle's medium (DMEM) containing 10% fetal bovine serum (FBS), 100 U/mL penicillin, and 100 µg/mL streptomycin (Sigma-Aldrich, St. Louis, MO, USA). Primary human umbilical vein endothelial cells (HUVECs) were purchased from ScienCell Research Laboratories (Carlsbad, CA, USA) and cultured in Endothelial Cell Medium (ScienCell Research Laboratories) supplemented with 10% FBS at 37°C in a humidified atmosphere with 5% CO₂. HUVECs at passages 3-8 were used in this study.

Plasmid construction and transfection

A fragment containing human miR-454 precursor was amplified from genomic DNA by PCR and cloned into pSuper vector (OligoEngine, Seattle, WA, USA). The complete coding region of *LRP6* gene was amplified by PCR using human *LRP6* cDNA (OriGene, Rockville, MD, USA) as a template and inserted into pcDNA3.1 (+) vector (Thermo Fisher Scientific, Carlsbad, CA, USA). The full-length *LRP6* 3'-UTR was amplified by PCR and inserted into the pGL3 plasmid (Promega, Madison, WI, USA). The mutated *LRP6* 3'-UTR reporter construct was generated by site-directed mutagenesis (QuikChange, Stratagene, La Jolla, CA, USA). All constructs were confirmed by sequencing.

PANC-1 and MiaPaCa-2 cells were seeded 16 h before transfection and transiently transfected with pSuper-miR-454 or empty vector, in some cases together with pcDNA3.1-LRP6, using Lipofectamine 2000 (Invitrogen, Carlsbad, CA, USA). At 24 h posttransfection, transfected

cells were tested for cell proliferation, invasion, and pro-angiogenic activity. For generation of stable clones, PANC-1 cells transfected with pSuper-miR-454 or empty vector were selected in the presence of puromycin (2 µg/mL; Sigma-Aldrich) for 5 days.

Quantitative real-time PCR (qRT-PCR) analysis

Total RNA was extracted from cells using Trizol reagent (Invitrogen) and reverse transcribed using the TaqMan miRNA Reverse Transcription Kit (Applied Biosystems, Foster City, CA, USA). Mature miR-454 and U6 (an internal control) levels were quantified by qRT-PCR using the TaqMan MicroRNA Assay Kit (Applied Biosystems). For detection of VEGF mRNA, real-time PCR was carried out using the iScript One-Step RT-PCR Kit with SYBR Green following the manufacturer's instructions (Bio-Rad Laboratories, Hercules, CA, USA). PCR primers are as follows [12]: VEGF forward 5'-TCTACCTCCACCATGCCAAGT-3' and VEGF reverse 5'-GATGATTCTGCCCTCCTCCTT-3'; β-actin forward 5'-TCAAGATCATTGCTCCTCCTG-3' and β-actin reverse 5'-CTGCTTGCTGATCCACATCTG-3'. The VEGF mRNA level was normalized to that of β-actin.

MTT assay

Cells transfected with indicated constructs were plated onto 96-well plates at 5×10^3 cells/well and cultured for 48 or 72 h. The 3-(4,5-dimethylthiazol-2-yl)-2,5-diphenyltetrazolium bromide (MTT) solution (0.5 mg/mL; Sigma-Aldrich) was added to each well. After incubation for 4 h at 37°C, dimethyl sulfoxide (Sigma-Aldrich) was added. Absorbance was recorded at 570 nm.

Colony formation assay

Cells transfected with indicated constructs were seeded onto 6-well plates at 600 cells/well and allowed to grow for 10 days to form colonies. Colonies were stained with 0.1% crystal violet (Jiancheng, Nanjing, China) for counting.

Cell cycle analysis

Cells were harvested, washed, and fixed with 70% ethanol overnight at 4°C. Afterwards, the cells were incubated with staining solution containing 50 µg/ml propidium iodide (PI) and 100 µg/ml of RNase A (Sigma-Aldrich) for 30 min in

the dark. Cell cycle distribution was analyzed using a flow cytometer.

In vitro invasion assay

Transwell invasion chambers pre-coated with Matrigel (BD Biosciences, San Jose, CA, USA) were used. Cells transfected with indicated constructs were seeded onto the top chamber 24 h after transfection at a density of 4×10^4 cells/well in 24-well plates. The lower chamber was filled with fresh medium containing 10% FBS. The cells were allowed to invade through the Matrigel membrane for 24 h. Invaded cells were stained with 0.1% crystal violet and counted in 5 random microscopic fields for each well.

Conditioned medium from tumor cells

PANC-1 cells stably transfected with the miR-454-expressing plasmid or vector were seeded onto 6-well plates (1×10^6 cells/well) and cultured in fresh DMEM containing 10% FBS to reach confluence. Afterwards, the medium was replaced by serum-free medium and incubated for 24 h. The conditioned medium was centrifuged for 10 min at 3,000 g at 4°C. The supernatant was filtered through a 0.22- μ m membrane and stored at -20°C until use.

In vitro capillary tube formation assay

In vitro HUVEC tube formation assay was performed as described previously [13]. Briefly, HUVECs (5×10^4 cells/well) were plated onto Matrigel-coated 24-well plates and cultured in fresh DMEM or conditioned medium. After 24 h of incubation, capillary-like structures were photographed. The cumulative tube length was quantified from 5 random microscopic fields.

Enzyme-linked immunosorbent assay (ELISA)

The concentration of VEGF protein in tumor cell conditioned medium was quantified using a VEGF ELISA Kit, according to the manufacturer's protocol (R&D Systems, Minneapolis, MN, USA).

Western blot analysis

Cells were lysed in lysis buffer (50 mmol/l Tris-HCl, pH 7.4; 150 mmol/l NaCl; 1% NP-40 and 0.5% sodium deoxycholate) with proteinase inhibitors (Beyotime, Haimen, China). Protein concentration was determined using the BCA

Protein Assay Kit (Beyotime). Protein samples (40 μ g per lane) were separated by SDS-PAGE and transferred onto nitrocellulose membranes. The membranes were probed with rabbit anti-non-phospho (active) β -catenin monoclonal antibody (#8814; Cell Signaling Technology, Danvers, MA, USA), rabbit anti-total β -catenin polyclonal antibody (#9562; Cell Signaling Technology), rabbit anti-LRP6 monoclonal antibody (#3395; Cell Signaling Technology), and rabbit anti- β -actin monoclonal antibody (#4970; Cell Signaling Technology) at 4°C overnight. These primary antibodies were diluted at 1:400. The membranes were then incubated for 1 h at room temperature with horseradish peroxidase-conjugated goat anti-rabbit IgG (1:2000 dilution; Santa Cruz Biotechnology, Santa Cruz, CA, USA). Protein signals were developed using the Amersham ECL Western Blotting Detection Reagent (GE Healthcare Life Sciences, Pittsburgh, PA, USA). Densitometric analysis was conducted using Quantity One software (version 4-2; Bio-Rad Laboratories).

Luciferase reporter assays

PANC-1 cells were seeded onto 24-well plates at 5×10^4 cells/well and transfected with pGL3-LRP6-3'-UTR (wild-type or mutated; 200 ng) and pSuper-miR-454 or empty vector (500 ng). The pRL-TK plasmid with constitutive expression of *Renilla* luciferase (Promega; 20 ng) was co-transfected to control for transfection efficiency. To assess β -catenin/TCF-driven transcriptional activity, miR-454-overexpressing PANC-1 cells were transfected with 300 ng pGL3-TopFlash or pGL3-FopFlash (Promega) and pRL-TK (10 ng) using Lipofectamine 2000. Relative luciferase activity was measured 24 h after transfection using the Dual-luciferase Reporter Assay Kit (Promega) according to the manufacturer's instructions.

Animal studies

Five-week-old male Balb/c nude mice were purchased from Shanghai Laboratory Animal Center (Shanghai, China) and randomly assigned to 2 groups (n = 10): control group and miR-454 group. For metastasis study, PANC-1 cells stably transfected with the miR-454-expressing plasmid or vector were injected via tail vein (2×10^6 cells/mouse), as described previously [14]. Animals were killed

miR-454 inhibits PDAC metastasis

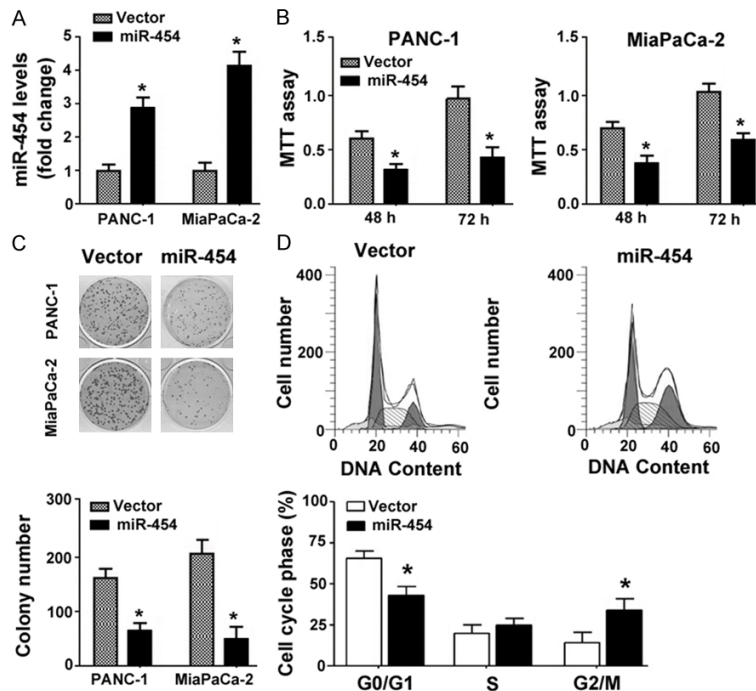


Figure 1. miR-454 exerts growth-suppressive effects on PDAC cells. A. qRT-PCR analysis of miR-454 levels in PDAC cells transfected with the miR-454-expressing plasmid or vector. B. PDAC cells transfected with the miR-454-expressing plasmid or vector were cultured for 48 or 72 h and tested for viability by MTT assays. C. Colony formation assay. Transfected cells were plated at a low density and allowed to form colonies for 10 days. Ectopic expression of miR-454 significantly inhibited colony formation of PDAC cells. *Top*, representative wells of the colonies. D. Analysis of cell cycle distribution by flow cytometry after PI staining. miR-454 overexpression led to an accumulation of cells at the G2/M phase in PANC-1 cells. *Top*, representative flow cytometry histograms showing cell cycle distribution. * $P < 0.05$ vs. vector-transfected cells.

at 8 weeks after cell inoculation. Lung tissues were removed and examined macroscopically for metastatic lesions. For histological analysis, lung tissue samples were fixed with 4% paraformaldehyde, embedded in paraffin, and sectioned. Tissue sections were stained with hematoxylin and eosin (H&E). All animal experiments were performed in accordance with institutional guidelines for the care and use of animals and approved by the Institutional Animal Care and Use Committee of Fudan University (Shanghai, China).

Statistical analysis

Data are presented as a mean \pm standard deviation and were analyzed by the Student's *t* test or one-way analysis of variance (ANOVA) with the Tukey test. The incidence of lung metastasis was compared using the Fisher's exact test.

P -value < 0.05 indicates statistically significant.

Results

miR-454 exerts growth-suppressive effects on PDAC cells

qRT-PCR analysis confirmed the restoration of miR-454 in PDAC cells transfected with the miR-454-expressing plasmid (Figure 1A). MTT assays showed that overexpression of miR-454 significantly inhibited the proliferation of PANC-1 and MiaPaCa-2 cells, compared to vector-transfected cells ($P < 0.05$; Figure 1B). Colony formation assays further demonstrated that ectopic expression of miR-454 led to 52% and 70% reduction in colony number in PANC-1 and MiaPaCa-2 cells, respectively, after culturing for 10 days (Figure 1C). Analysis of cell cycle distribution by flow cytometry revealed that miR-454-overexpressing PANC-1 cells displayed an accumulation of cells at the G2/M phase (Figure 1D). In contrast, the percentage of cells

at the G0/G1 phase was significantly decreased in miR-454-overexpressing cells, indicating a G2/M cell cycle arrest.

Overexpression of miR-454 suppresses the invasive and pro-angiogenic potential of PDAC cells

As determined by Matrigel-coated invasion assays, overexpression of miR-454 significantly decreased the number of PANC-1 invading cells through Matrigel membranes by 63% ($P < 0.05$ vs. vector-transfected cells; Figure 2A). Similarly, miR-454-overexpressing MiaPaCa-2 cells showed significantly less invasiveness than control cells ($P < 0.05$; Figure 2A). To assess the pro-angiogenic activity of miR-454-overexpressing PDAC cells, conditioned media from transfected PANC-1 cells were collected and used to stimulate HUVECs to form

miR-454 inhibits PDAC metastasis

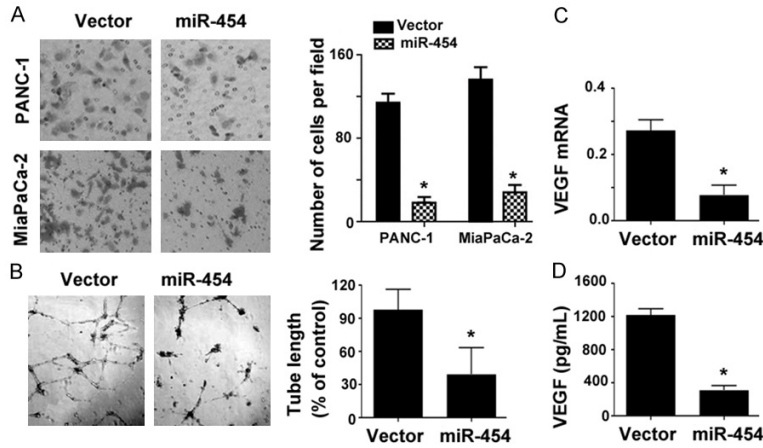


Figure 2. Overexpression of miR-454 suppresses the invasive and pro-angiogenic potential of PDAC cells. A. Matrigel-coated invasion assays. miR-454 overexpression significantly inhibited the invasiveness of PDAC cells. *Left*, representative images of transwell invasion assays. B. Capillary tube-like structure formation. Conditioned media from transfected PANC-1 cells were incubated with HUVECs and tube-like structures were examined. *Left*, representative photomicrographs of tube-like structures. C. qRT-PCR analysis of VEGF mRNA levels in PANC-1 cells transfected with the miR-454-expressing plasmid or vector. D. Measurement of VEGF protein levels in conditioned media from transfected PANC-1 cells by ELISA. * $P < 0.05$ vs. vector-transfected cells.

miR-454 group significantly inhibited the formation of tubes (**Figure 2B**). We further examined the effect of miR-454 overexpression on VEGF production. As expected, the transcription and secretion of VEGF was significantly suppressed in miR-454-overexpressing PANC-1 cells (**Figure 2C** and **2D**).

miR-454 inhibits Wnt/ β -catenin signaling in PDAC cells by targeting LRP6

Bioinformatic analysis using the TargetScan algorithm (http://www.targetscan.org/vert_71/) suggested that LRP6 was a potential target gene of miR-454 (**Figure 3A**). Luciferase reporter assays confirmed that co-transfection with the miR-454-expressing plasmid resulted in a significant repression of the reporter containing the 3'-UTR of LRP6 mRNA, but not the mutated LRP6 3'-UTR (**Figure 3B**). Consistently, Western blot analysis revealed a marked downregulation of endogenous LRP6 in miR-454-overexpressing PANC-1 and MiaPaCa-2 cells (**Figure 3C**). Since LRP6 is an important regulator of Wnt/ β -catenin signaling [15], we tested whether miR-454 overexpression affected the activation of Wnt/ β -catenin signaling in PDAC cells. As shown in **Figure 3C**, the levels of hypophosphorylated, active β -catenin were remarkably lower in miR-454-overexpressing PDAC cells than in control counterparts. Moreover, overexpression of miR-454 significantly inhibited the activity of

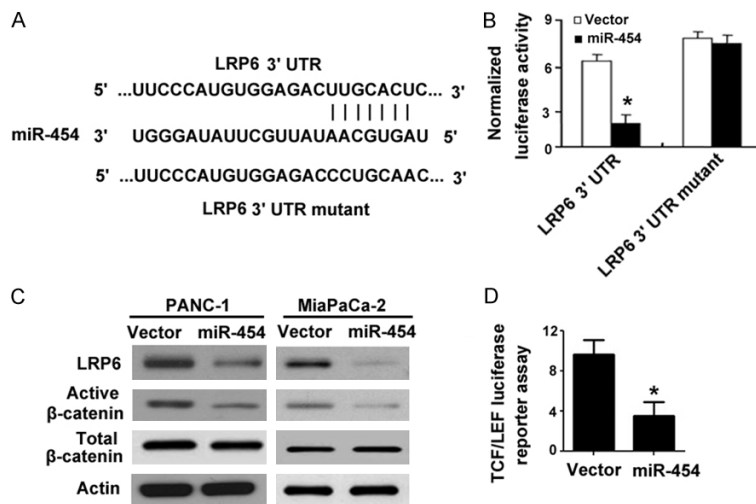


Figure 3. miR-454 inhibits Wnt/ β -catenin signaling in PDAC cells by targeting LRP6. A. Bioinformatic analysis using the TargetScan algorithm (http://www.targetscan.org/vert_71/) suggested that miR-454 could target the 3'-UTR of LRP6 mRNA. B. Luciferase reporter assays. Delivery of miR-454 could inhibit the expression of the reporter containing the 3'-UTR of LRP6 mRNA, but not the mutated LRP6 3'-UTR. C. Western blot analysis of indicated proteins in PDAC cells transfected with the miR-454-expressing plasmid or vector. D. TCF/LEF luciferase reporter assays. Overexpression of miR-454 significantly suppressed the activity of the TCF/LEF luciferase reporter in PANC-1 cells. * $P < 0.05$ vs. vector-transfected cells.

capillary tube-like structures. Notably, we found that addition of conditioned media from the

the TCF/LEF luciferase reporter in PANC-1 cells (**Figure 3D**). Taken together, miR-454 can tar-

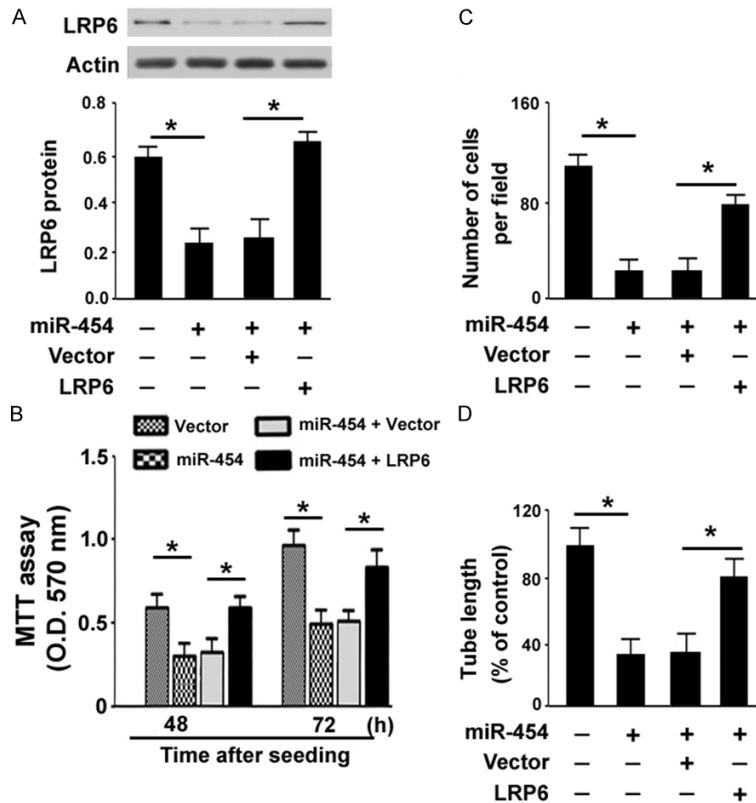


Figure 4. Enforced expression of LRP6 reverses the suppressive effects of miR-454 on PDAC cells. **A.** Western blot analysis of LRP6 in PANC-1 cells transfected with indicated constructs. **B.** MTT assays were performed to determine the viability of PANC-1 cells transfected with indicated constructs after culturing for 48 or 72 h. **C.** Matrigel-coated invasion assays. PANC-1 cells were transfected with indicated constructs and examined for the invasiveness. **D.** Capillary tube-like structure formation. Conditioned media from transfected PANC-1 cells were incubated with HUVECs and the length of tube-like structures was measured. * $P < 0.05$.

get LRP6 to suppress Wnt/ β -catenin activation in PDAC cells.

Enforced expression of LRP6 reverses the suppressive effects of miR-454 on PDAC cells

To test the hypothesis that downregulation of LRP6 is required for the action of miR-454 in PDAC cells, we overexpressed a miRNA-resistant variant of LRP6 in PANC-1 cells with overexpression of miR-454 (Figure 4A). Of note, miR-454-expressing PANC-1 cells co-transfected with the LRP6 construct exhibited significantly higher proliferation (Figure 4B) and invasion (Figure 4C) than those co-transfected with empty vector. Moreover, the pro-angiogenic activity of miR-454-overexpressing PANC-1 cells was partially restored upon ectopic expression of LRP6 (Figure 4D). These data indicate that the tumor-suppressive activity of

miR-454 is associated with repression of LRP6.

miR-454 inhibit tumor metastasis to the lung in vivo

Finally, we checked whether miR-454 could inhibit PDAC metastasis in vivo. To this end, PANC-1 cells stably transfected with the miR-454-expressing plasmid or vector were injected to the tail veins of nude mice. Lung metastasis was detected in 7 out of 10 mice injected with vector-transfected cells and 2 out of 10 mice injected with miR-454-overexpressing cells ($P = 0.0349$; Figure 5A and 5B). H&E staining of lung tissue sections (Figure 5C and 5D) confirmed that the number of lung micrometastatic lesions was significantly lower in the miR-454 group than in the control group (6.2 ± 1.5 vs. 28.4 ± 3.6 ; $P < 0.05$). These results indicate the anti-metastatic potential of miR-454 in PDAC.

Discussion

Our previous work showed that miR-454 can inhibit PDAC growth by interfering with the recruitment of macrophages [11]. Tumor-associated macrophages contribute to the establishment of a tumor-favorable microenvironment [16, 17]. Therefore, it was suggested that miR-454 has the ability to modulate the tumor microenvironment in PDAC. Since this miRNA has been documented to promote cancer cell proliferation and invasion in several cancer types [9, 10], in the present study we tested the hypothesis that miR-454 might affect multiple aspects of the biology of PDAC. In support of this hypothesis, we noted that restoration of miR-454 significantly inhibited the proliferation and colony formation of PDAC cells. Consistently, miR-454 overexpression was found to arrest PDAC cells at the G2/M phase. Apart from inhibition of cell growth, overexpression of miR-454 also impaired the invasion and pro-angiogenic poten-

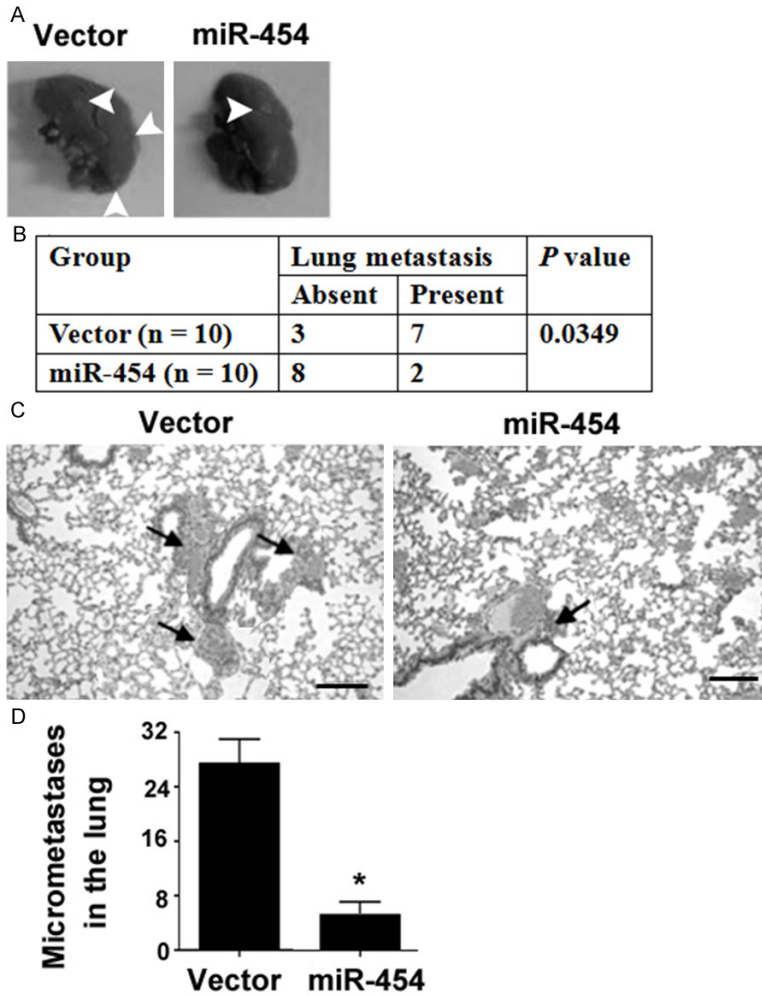


Figure 5. miR-454 inhibit tumor metastasis to the lung in vivo. **A.** Representative photographs of the metastatic lesions (indicated by arrowhead) in the lung. **B.** Comparison of the incidences of lung metastasis between the vector and miR-454 groups by the Fisher's exact test. **C.** H&E staining of lung tissue sections revealed micrometastatic lesions (indicated by arrow). Scale bar = 150 μ m. **D.** Bar graphs showing quantification of lung micrometastatic lesions. * $P < 0.05$ vs. the vector group.

tial of PDAC cells. Angiogenesis is a fundamental process for tumor growth and progression [2]. Tumor cells produce a number of growth factors and cytokines, which can modulate angiogenesis of endothelial cells [18, 19]. In this study, we showed that enforced expression of miR-454 resulted in a significant decline in the expression and secretion of VEGF in PDAC cells, which provides an explanation for the reduced pro-angiogenic activity of miR-454-overexpressing PDAC cells. Taken together, miR-454 functions as a tumor suppressor in PDAC. However, this miRNA exerts tumor-promoting effects on several other cancers such as uveal melanoma [9] and non-small cell lung

cancer [10], suggesting its context-dependent functions.

To determine the mechanism by which miR-454 exerts its suppressive activity in PDAC, we performed bioinformatic analysis and luciferase reporter assays and identified LRP6 as a direct target gene of miR-454. Overexpression of miR-454 led to a significant inhibition of endogenous LRP6 expression in PDAC cells. Interestingly, LRP6 has the capacity to promote tumor growth and metastasis via the Wnt/ β -catenin pathway [15, 20]. It has been reported that miR-126 suppresses the growth of papillary thyroid carcinoma by targeting LRP6 [21]. Similarly, biochemical inhibition of LRP6 was shown to inhibit PDAC growth, which was accompanied by inactivation of Wnt/ β -catenin signaling [22]. These studies encourage us to hypothesize that miR-454 might exert its suppressive activity by inhibiting Wnt/ β -catenin signaling via downregulation of LRP6. In support of this hypothesis, reduced β -catenin-dependent transcriptional activity was noted in miR-454-overexpressing PDAC cells. Rescue experiments provided additional evidence that downregulation of LRP6 contributes to the suppressive activity of miR-454 in the growth, invasion, and angiogenesis in PDAC. It should be mentioned that miR-454 can also downregulate target genes other than LRP6, e.g. c-Met [23]. A previous study reported that miR-454 can restrict the growth and invasion of osteosarcoma cells by targeting c-Met [23]. Therefore, it is possible that other undefined target genes may also mediate the activity of miR-454 in PDAC.

Distant metastasis is regarded as a major cause of cancer-related deaths [24]. To complete our previous report showing the growth-suppressive activity of miR-454 [11], the pres-

ent study demonstrated that miR-454 over-expression hampered the metastatic growth of PDAC cells in the lung in mouse models. The in vivo findings are also consistent with the Transwell invasion experiments. Restoration of miR-454 may thus represent a potential therapeutic strategy for controlling PDAC metastasis.

In conclusion, miR-454 exhibits suppressive activity in growth, metastasis, and angiogenesis in PDAC. Targeting LRP6 and subsequent inactivation of Wnt/ β -catenin signaling represents a novel mechanism for the action of miR-454. These observations provide a rationale to investigate the therapeutic benefits of delivery of miR-454 in the treatment of PDAC.

Disclosure of conflict of interest

None.

Address correspondence to: Tiantao Kuang, Department of General Surgery, Zhongshan Hospital, Fudan University, Shanghai 200032, China. E-mail: WwHY7890667@163.com

References

- [1] Michl P, Gress TM. Current concepts and novel targets in advanced pancreatic cancer. *Gut* 2013; 62: 317-326.
- [2] Popescu AM, Purcaru SO, Alexandru O, Dricu A. New perspectives in glioblastoma antiangiogenic therapy. *Contemp Oncol (Pozn)* 2016; 20: 109-118.
- [3] Georgiadou D, Sergeantanis TN, Sakellariou S, Filippakis GM, Zagouri F, Vlachodimitropoulos D, Psaltopoulou T, Lazaris AC, Patsouris E, Zografos GC. VEGF and Id-1 in pancreatic adenocarcinoma: prognostic significance and impact on angiogenesis. *Eur J Surg Oncol* 2014; 40: 1331-1337.
- [4] Solorzano CC, Baker CH, Bruns CJ, Killion JJ, Ellis LM, Wood J, Fidler IJ. Inhibition of growth and metastasis of human pancreatic cancer growing in nude mice by PTK 787/ZK222584, an inhibitor of the vascular endothelial growth factor receptor tyrosine kinases. *Cancer Biother Radiopharm* 2001; 16: 359-370.
- [5] Fukasawa M, Korc M. Vascular endothelial growth factor-trap suppresses tumorigenicity of multiple pancreatic cancer cell lines. *Clin Cancer Res* 2004; 10: 3327-3332.
- [6] Srivastava S, Tsongalis GJ, Kaur P. Role of microRNAs in regulation of the TNF/TNFR gene superfamily in chronic lymphocytic leukemia. *Clin Biochem* 2016; 49: 1307-1310.
- [7] Wang C, Liu P, Wu H, Cui P, Li Y, Liu Y, Liu Z, Gou S. MicroRNA-323-3p inhibits cell invasion and metastasis in pancreatic ductal adenocarcinoma via direct suppression of SMAD2 and SMAD3. *Oncotarget* 2016; 7: 14912-14924.
- [8] Fan P, Liu L, Yin Y, Zhao Z, Zhang Y, Amponsah PS, Xiao X, Bauer N, Abukiwan A, Nwaeburu CC, Gladkich J, Gao C, Schemmer P, Gross W, Herr I. MicroRNA-101-3p reverses gemcitabine resistance by inhibition of ribonucleotide reductase M1 in pancreatic cancer. *Cancer Lett* 2016; 373: 130-137.
- [9] Sun L, Wang Q, Gao X, Shi D, Mi S, Han Q. MicroRNA-454 functions as an oncogene by regulating PTEN in uveal melanoma. *FEBS Lett* 2015; 589: 2791-2796.
- [10] Zhu DY, Li XN, Qi Y, Liu DL, Yang Y, Zhao J, Zhang CY, Wu K, Zhao S. MiR-454 promotes the progression of human non-small cell lung cancer and directly targets PTEN. *Biomed Pharmacother* 2016; 81: 79-85.
- [11] Fan Y, Xu LL, Shi CY, Wei W, Wang DS, Cai DF. MicroRNA-454 regulates stromal cell derived factor-1 in the control of the growth of pancreatic ductal adenocarcinoma. *Sci Rep* 2016; 6: 22793.
- [12] Tang XD, Zhou X, Zhou KY. Dauricine inhibits insulin-like growth factor-I-induced hypoxia inducible factor 1 α protein accumulation and vascular endothelial growth factor expression in human breast cancer cells. *Acta Pharmacol Sin* 2009; 30: 605-616.
- [13] Duan Y, Wu X, Zhao Q, Gao J, Huo D, Liu X, Ye Z, Dong X, Fu Z, Shang Y, Xuan C. DOT1L promotes angiogenesis through cooperative regulation of VEGFR2 with ETS-1. *Oncotarget* 2016; 7: 69674-69687.
- [14] Anderson M, Marayati R, Moffitt R, Yeh JJ. Hexokinase 2 promotes tumor growth and metastasis by regulating lactate production in pancreatic cancer. *Oncotarget* 2016; [Epub ahead of print].
- [15] Schmitt M, Metzger M, Gradl D, Davidson G, Orian-Rousseau V. CD44 functions in Wnt signaling by regulating LRP6 localization and activation. *Cell Death Differ* 2015; 22: 677-689.
- [16] Nielsen SR, Quaranta V, Linford A, Emeagi P, Rainer C, Santos A, Ireland L, Sakai T, Sakai K, Kim YS, Engle D, Campbell F, Palmer D, Ko JH, Tuveson DA, Hirsch E, Mielgo A, Schmid MC. Macrophage-secreted granulins support pancreatic cancer metastasis by inducing liver fibrosis. *Nat Cell Biol* 2016; 18: 549-560.
- [17] Miyake M, Hori S, Morizawa Y, Tatsumi Y, Nakai Y, Anai S, Torimoto K, Aoki K, Tanaka N, Shimada K, Konishi N, Toritsuka M, Kishimoto T, Rosser CJ, Fujimoto K. CXCL1-mediated interaction of cancer cells with tumor-associated macrophages and cancer-associated fibro-

miR-454 inhibits PDAC metastasis

- blasts promotes tumor progression in human bladder cancer. *Neoplasia* 2016; 18: 636-646.
- [18] He T, Qi F, Jia L, Wang S, Wang C, Song N, Fu Y, Li L, Luo Y. Tumor cell-secreted angiogenin induces angiogenic activity of endothelial cells by suppressing miR-542-3p. *Cancer Lett* 2015; 368: 115-125.
- [19] Cao Z, Ding BS, Guo P, Lee SB, Butler JM, Casey SC, Simons M, Tam W, Felsher DW, Shido K, Rafii A, Scandura JM, Rafii S. Angiocrine factors deployed by tumor vascular niche induce B cell lymphoma invasiveness and chemoresistance. *Cancer Cell* 2014; 25: 350-365.
- [20] Ren DN, Chen J, Li Z, Yan H, Yin Y, Wo D, Zhang J, Ao L, Chen B, Ito TK, Chen Y, Liu Z, Li Y, Yang J, Lu X, Peng Y, Pan L, Zhao Y, Liu S, Zhu W. LRP5/6 directly bind to frizzled and prevent frizzled-regulated tumour metastasis. *Nat Commun* 2015; 6: 6906.
- [21] Wen Q, Zhao J, Bai L, Wang T, Zhang H, Ma Q. miR-126 inhibits papillary thyroid carcinoma growth by targeting LRP6. *Oncol Rep* 2015; 34: 2202-2210.
- [22] Arensman MD, Nguyen P, Kershaw KM, Lay AR, Ostertag-Hill CA, Sherman MH, Downes M, Liddle C, Evans RM, Dawson DW. Calcipotriol targets LRP6 to inhibit Wnt signaling in pancreatic cancer. *Mol Cancer Res* 2015; 13: 1509-1519.
- [23] Niu G, Li B, Sun J, Sun L. miR-454 is down-regulated in osteosarcomas and suppresses cell proliferation and invasion by directly targeting c-Met. *Cell Prolif* 2015; 48: 348-355.
- [24] Wang L, Bai YY, Yang Y, Hu F, Wang Y, Yu Z, Cheng Z. Diabetes mellitus stimulates pancreatic cancer growth and epithelial-mesenchymal transition-mediated metastasis via a p38 MAPK pathway. *Oncotarget* 2016; 7: 38539-38550.